


RESEARCH

Open Access



# Application of diffusion tensor imaging in Alzheimer's disease: quantification of white matter microstructural changes

Shereen Magdy Abdel Malak Esrael<sup>1,2\*</sup> , Ahmed Mostafa Mohamed Hamed<sup>1</sup>, Eman M. Khedr<sup>3</sup> and Radwa Kamel Soliman<sup>1</sup>

## Abstract

**Background:** Alzheimer's disease (AD) is the most common cause of dementia in the aging population, responsible for 60–70% of all demented cases. Diffusion tensor imaging (DTI) is a very recent technique that allows the mapping of white matter (WM) microstructure changes in neurological disorders. The current study was conducted to compare DTI parameters between AD patients and healthy elderly subjects and to determine whether DTI can act as a potential biomarker for AD.

**Results:** There were significant differences in Modified Mini-Mental State Examination (MMSE) and Clinical Dementia Rating (CDR) between the two groups. As regards the DTI parameters, significant differences were found between AD patients versus healthy subjects, in the mean diffusivity (MD) of the splenium  $[(1.05 \pm 0.19) \text{ vs. } (0.92 \pm 0.22), P=0.03]$ , the MD of the right uncinate fasciculus  $[(0.92 \pm 0.04) \text{ vs. } (0.87 \pm 0.05), P=0.01]$ , and MD of the right arcuate fasciculus (AF)  $[(0.83 \pm 0.04) \text{ vs. } (0.79 \pm 0.04), P=0.01]$ , as well as the MD of the right and left inferior fronto-occipital fasciculus (IFOF)  $[(0.89 \pm 0.06) \text{ vs. } (0.83 \pm 0.04), P=0.01]$ . In addition, there were significant differences in the fractional anisotropy (FA) of the right and left cingulum between both groups  $[(0.45 \pm 0.02) \text{ vs. } (0.47 \pm 0.03), P=0.01]$  and  $(0.45 \pm 0.03) \text{ vs. } 0.49 \pm 0.04, P=0.01$ , respectively]. The overall accuracy of the aforementioned parameters ranged between 73 and 81% with the MD of the left cingulum revealing the highest accuracy.

**Conclusion:** DTI proved to be a useful tool in differentiating AD patients from healthy subjects. In our study, we found that the splenium, cingulum, IFOF, and the right UF and right AF are the main tracts involved in AD. The left cingulum provided the highest accuracy in differentiating AD from normal subjects.

**Keywords:** Alzheimer disease, Diffusion tensor imaging, Fractional anisotropy, Mean diffusivity

## Background

Alzheimer's disease (AD) is a progressive neurodegenerative disease representing the most prevalent cause of dementia in the elderly population, accounting for 60–70% of all demented cases [1]. In 2015, there were roughly 46 million people worldwide with AD [2]. It is

characterized by gradual cognitive impairment and memory loss that gradually cause severe disabilities and significant complications, eventually leading to death [3]. Histopathologically, AD is characterized by extracellular beta-amyloid protein and Tau protein intercellular aggregation (known as neurofibrillary tangles), which lead to the damage and destruction of neurons resulting in memory loss and other manifestations of Alzheimer disease [4].

Previous imaging researches focused on the damage of gray matter (GM) based on voxel-based morphometry and positron emission tomography [5]. While it was

\* Correspondence: [shereenmagdy160@gmail.com](mailto:shereenmagdy160@gmail.com)

<sup>1</sup>Department of Diagnostic and Interventional Radiology, Faculty of Medicine, Assiut University, Assiut, Egypt

<sup>2</sup>Department of Diagnostic Radiology, South Egypt Cancer Institute, Assiut University, Assiut, Egypt

Full list of author information is available at the end of the article

believed that AD is a GM disease, various structural MRI studies revealed variable degrees of WM abnormalities such as demyelination and gliosis [6]. This WM damage is thought to be secondary to the GM damage [7]. Good deals of evidences, however, indicate that WM damage is independent of GM damage. It may even precede the GM involvement, which indicates the primary role of WM in the pathology of AD [8]. Additionally, as Tau is primarily found in axons, it is possible that changes in WM microstructure may exist in the early stages of AD [9]. Changes in the WM microstructure can be quantified using diffusion tensor imaging (DTI). Therefore, DTI can be applied to quantify WM microstructure changes in AD [10].

DTI-MRI is a fairly new tool that enables mapping of WM microstructure changes in neurological disease. From the tensor, it is possible to derive the mean diffusivity (MD) that describe the overall mean-squared displacement of molecules which is the average of the diffusion ellipsoid size, and the fractional anisotropy (FA) which measures the fraction of the magnitude of diffusion that can be recognized to anisotropic diffusion. Those are the most robust measures of anisotropy which measure the degree of deviation from isotropic diffusion [11]. In this study, we aimed to compare DTI parameters between AD patients and healthy elderly subjects, to determine whether DTI can identify WM microstructural changes in AD patients and act as a potential biomarker for AD.

## Methods

A prospective cross-sectional study was conducted at the Diagnostic Radiology Department. It was performed in the period from May 2017 to May 2019.

### Subjects

A total of 16 Alzheimer patients (9 males and 7 females) were recruited, ranging from 63 to 86 years of age, with a mean education level of  $3.94 \pm 1.24$  years. Patients with AD were included after clinical neurological evaluation (according to the criteria of the National Institute of Neurological and Communicative Disorders and Stroke Alzheimer Disease and Related Disorders Association) [12].

In addition, 16 control subjects (9 males and 7 females), with normal memory and cognition with no history of neurological or psychiatric disorders, were included. Control subjects were matched with AD patients for age and education level, age range from 58 to 80 years, with a mean education level of  $5.06 \pm 1.24$  years.

All participants or their caregivers gave informed consent before participation in the investigation and after

the full explanation of the study protocol. The study was approved by the local ethical committee.

Exclusion criteria included patients with other types of dementia such as fronto-temporal dementia or any other factors causing dementia and patients with pyramidal or extrapyramidal tract signs. Any patient with moderate or profound subcortical ischemic changes, structural abnormalities in the brain and/or any metallic prosthesis was excluded.

### Neuropsychological assessment

For staging of dementia, patients were classified into mild, moderate, and severe AD according to Modified Mini-Mental State Examination (MMMSE) and Clinical Dementia Rating (CDR).

Each patient was evaluated with MMMSE by a trained neuropsychologist. It is a measure of global cognition, for assessing orientation, attention, language, and memory. The cutoff point  $\leq 23$  is used in order to detect suspected demented subjects. Dementia was classified according to the MMMSE score as 23–19, 18–11, and less than 11 for mild, moderate, and severe dementia, respectively, using the full score of 30 points in the case of educated patients [13].

The CDR is a numeric scale used to quantify the severity of symptoms of dementia. A structured interview protocol for the assessment of a patient's cognitive and functional performance in six areas was used: memory, orientation, judgment and problem solving, community affairs, home and hobbies, and personal care.

### MRI protocol

MRI examination was performed at a 1.5-T unit (Achieva, Phillips Healthcare) using the standard head coil for signal perception.

3D fluid-attenuated inversion recovery (FLAIR) images were acquired with FLAIR sequences (TR/TE = 11,000/140ms, matrix =  $208 \times 106$ , voxel size  $1 \times 1 \times 1$ mm). DTI was obtained using an echo-planar imaging sequence with a  $b$  value of  $1000 \text{ s/mm}^2$  and a  $b$  value of  $0 \text{ s/mm}^2$ , 32 uniform directions, and a matrix size of  $112 \times 112$  with a 2-mm isotropic spatial resolution. TR/TE is equal to 11,785/110 ms. The slice thickness was 2 mm. The examination time of this sequence was 13.33 min.

### Post-processing

After data preparation, images were transferred to the Philips Workstation software package; the 2 maps were obtained (FA and MD colored maps). Processing was performed on colored FA maps where 3D FLAIR was overlaid.

The color maps provide information about the orientation of the tracts, where red color indicates a latero-lateral direction (left to right and right to left), green

color an anterior-posterior direction (and vice versa), and blue color a dorsal-ventral direction (and vice versa). Other colors indicate intermediate orientations.

The following WM tracts were manually dissected using either single or two ROI (region of interest) approaches. Single ROI approach was used for the fornixes, anterior thalamic radiation (ATR), cingulum, and corpus callosum (genu, body, and splenium) [14]. Two ROI approaches were drawn for arcuate fasciculus (AF), uncinate fasciculus (UF), inferior longitudinal fasciculus (ILF), and inferior occipito-frontal fasciculus (IFOF) bilaterally [15, 16]. The tracts were dissected conjointly by two radiologists: a resident (SMA) with 4 years of experience and a consultant radiologist (RKS) with over 10 years of experience.

### Statistical analysis

Data was collected and analyzed using SPSS (Statistical Package for the Social Science, version 20, IBM, and Armonk, NY). Continuous data was expressed in the form of mean  $\pm$  SD while nominal data was expressed in the form of frequency (percentage).

The chi-squared test was used to compare the nominal data of different groups in the study while the Student *t* test was used to compare the mean of DTI parameters (FA and MD) of the selected WM tracts between AD patients and control subjects. The diagnostic performance of significant DTI parameters was determined by the ROC curve. The level of confidence was kept at 95%; hence, *P* value was significant if  $< 0.05$ .

### Results

The mean age of the study group was  $71.01 \pm 7.71$  years while the mean age of the control group was  $66.25 \pm 6.54$  years. It was noticed that the majority (56.2%) of both groups were males. The MMSE and CDR were significantly lower in AD patients compared to control subjects ( $P = 0.01$  and  $0.001$ , respectively) (baseline data of studied groups was shown in Table 1).

Differences in DTI parameters (FA and MD) of the examined tracts between AD and healthy controls are shown in Table 2. There was significant higher MD

values of the splenium in AD patients ( $1.05 \pm 0.19$  vs.  $0.92 \pm 0.22$ ;  $P = 0.03$ ). In addition, there were significant lower FA at the right cingulum ( $0.45 \pm 0.02$  vs.  $0.47 \pm 0.03$ ;  $P = 0.01$ ) and lower FA at the left cingulum ( $0.45 \pm 0.03$  vs.  $0.49 \pm 0.04$ ;  $P = 0.01$ ) in AD patients compared to healthy controls.

A significant higher MD at the right UF ( $0.92 \pm 0.04$  vs.  $0.87 \pm 0.05$ ;  $P = 0.01$ ), right AF ( $0.83 \pm 0.04$  vs.  $0.79 \pm 0.04$ ;  $P = 0.01$ ), right IFOF ( $0.91 \pm 0.07$  vs.  $0.85 \pm 0.04$ ;  $P = 0.01$ ), and left IFOF ( $0.89 \pm 0.06$  vs.  $0.83 \pm 0.04$ ;  $P = 0.01$ ) was observed in AD patients. Otherwise, there were no significant differences as regards the other examined tracts between the patients and the control group.

Figure 1 shows an example of the examined tracts of AD patients vs. healthy controls.

Diagnostic performance DTI parameters (MD and FA) of the examined tracts are shown in (Fig. 2). MD of the splenium at a cutoff point of 0.961 with an AUC of 0.75 had 69% sensitivity and 81% specificity for the diagnosis of AD with an accuracy of 77.3% (Fig. 2a).

FA of the right cingulum, best differentiated between AD and control groups, at a cutoff point of  $< 0.469$  (AUC = 0.74) with a sensitivity of 87.5%, a specificity of 62.5% and an accuracy of 77.3%, while FA of the left cingulum, differentiated the two groups, at a cutoff point of  $< 0.477$  (AUC = 0.73) with a sensitivity of 69%, a specificity of 75% and an accuracy of 88.8% (Fig. 2b).

In addition, MD of the right UF, best discriminated AD from control groups, at a cutoff point of  $> 0.876$  (AUC of = 0.74) with a sensitivity of 94%, a specificity of 50%, and an accuracy of 73% (Fig. 2c). MD of the right AF, however, discriminated the two groups, at a cutoff point of  $> 0.78$  (AUC = 0.76) with a sensitivity of 87.5%, a specificity of 56.3%, and an accuracy of 73% (Fig. 2d).

Furthermore, MD of the right IFOF, best differentiated between AD and control groups, at a cutoff point of  $> 0.88$  (AUC of = 0.88) with a sensitivity of 75%, a specificity of 63% and an accuracy of 68.2%, while MD of the left IFOF, discriminated the two groups, at a cutoff point of  $> 0.82$  (AUC of = 0.82) had 100% with a sensitivity of

**Table 1** Baseline data of studied groups

	Study group (n= 16)	Control group (n= 16)	P value
Age (years)	71.01 $\pm$ 7.71	66.25 $\pm$ 6.54	0.07
Sex	9 (56.2%)	9 (56.2%)	0.63
Male	7 (43.8%)	7 (43.8%)	
Female			
Education years	3.94 $\pm$ 1.24	5.06 $\pm$ 1.24	0.59
MMSE	15.02 $\pm$ 5.47	27.54 $\pm$ 1.50	0.01
CDR	2.062 $\pm$ 0.7	1	< 0.001

Data expressed as frequency (percentage), mean (SD). *P* value was significant if  $< 0.05$

MMSE Mini-Mental State Examination, CDR Clinical Dementia Rating

**Table 2** DTI parameters of the corpus callosum, cingulum, fornix, anterior thalamic radiation, AF, ILF, IFOF, and UF in the studied groups

	Study group (n= 16)	Control group (n= 16)	P
<b>Corpus callosum genu</b>	0.52 ± 0.04	0.53 ± 0.03	0.43
FA	0.91 ± 0.09	0.87 ± 0.10	0.30
MD			
<b>Body</b>	0.53 ± 0.04	0.55 ± 0.05	0.34
FA	0.94 ± 0.24	0.91 ± 0.16	0.57
MD			
<b>Splenium</b>	0.56 ± 0.14	0.61 ± 0.05	0.15
FA	1.05 ± 0.19	0.92 ± 0.22	<b>0.03</b>
MD			
<b>Right cingulum</b>	0.45 ± 0.02	0.47 ± 0.03	<b>0.01</b>
FA	0.85 ± 0.04	0.83 ± 0.06	0.29
MD			
<b>Left cingulum</b>	0.45 ± 0.03	0.49 ± 0.04	<b>0.01</b>
FA	0.86 ± 0.05	0.82 ± 0.06	0.07
MD			
<b>Right FNX</b>	0.33 ± 0.05	0.36 ± 0.04	0.14
FA	1.49 ± 0.40	1.45 ± 0.23	0.77
MD			
<b>Left FNX</b>	0.34 ± 0.04	0.36 ± 0.04	0.22
FA	1.60 ± 0.38	1.50 ± 0.28	0.47
MD			
<b>Right ATR</b>	0.43 ± 0.04	0.44 ± 0.05	0.61
FA	0.91 ± 0.17	0.82 ± 0.08	0.07
MD			
<b>Left ATR</b>	0.43 ± 0.04	0.45 ± 0.05	0.14
FA	0.89 ± 0.08	0.83 ± 0.12	0.09
MD			
<b>Right AF</b>	0.45 ± 0.02	0.46 ± 0.02	0.34
FA	0.83 ± 0.04	0.79 ± 0.04	<b>0.01</b>
MD			
<b>Left AF</b>	0.46 ± 0.02	0.47 ± 0.03	0.47
FA	0.81 ± 0.05	0.79 ± 0.04	0.29
MD			
<b>Right ILF</b>	0.45 ± 0.03	0.47 ± 0.03	0.13
FA	0.89 ± 0.04	0.90 ± 0.22	0.86
MD			
<b>Left ILF</b>	0.45 ± 0.04	0.47 ± 0.04	0.18
FA	0.88 ± 0.03	0.90 ± 0.13	0.68
MD			
<b>Right IFOF</b>	0.46 ± 0.02	0.46 ± 0.03	0.80
FA	0.91 ± 0.07	0.85 ± 0.04	<b>0.01</b>
MD			
<b>Left IFOF</b>	0.47 ± 0.03	0.48 ± 0.02	0.23
FA	0.89 ± 0.06	0.83 ± 0.04	<b>0.01</b>
MD			
<b>Right UF</b>	0.38 ± 0.02	0.39 ± 0.03	0.28
FA	0.92 ± 0.04	0.87 ± 0.05	<b>0.01</b>
MD			
<b>Left UF</b>	0.37 ± 0.03	0.39 ± 0.03	0.11
FA	0.88 ± 0.21	0.90 ± 0.10	0.79
MD			

Data expressed as mean (SD). P value was significant if &lt; 0.05

FA fractional anisotropy, MD mean diffusivity, DTI diffusion tensor imaging, FNX fornix, ATR anterior thalamic radiation, AF arcuate fasciculus, ILF inferior longitudinal fasciculus, IFOF inferior fronto-occipital fasciculus, UF uncinate fasciculus

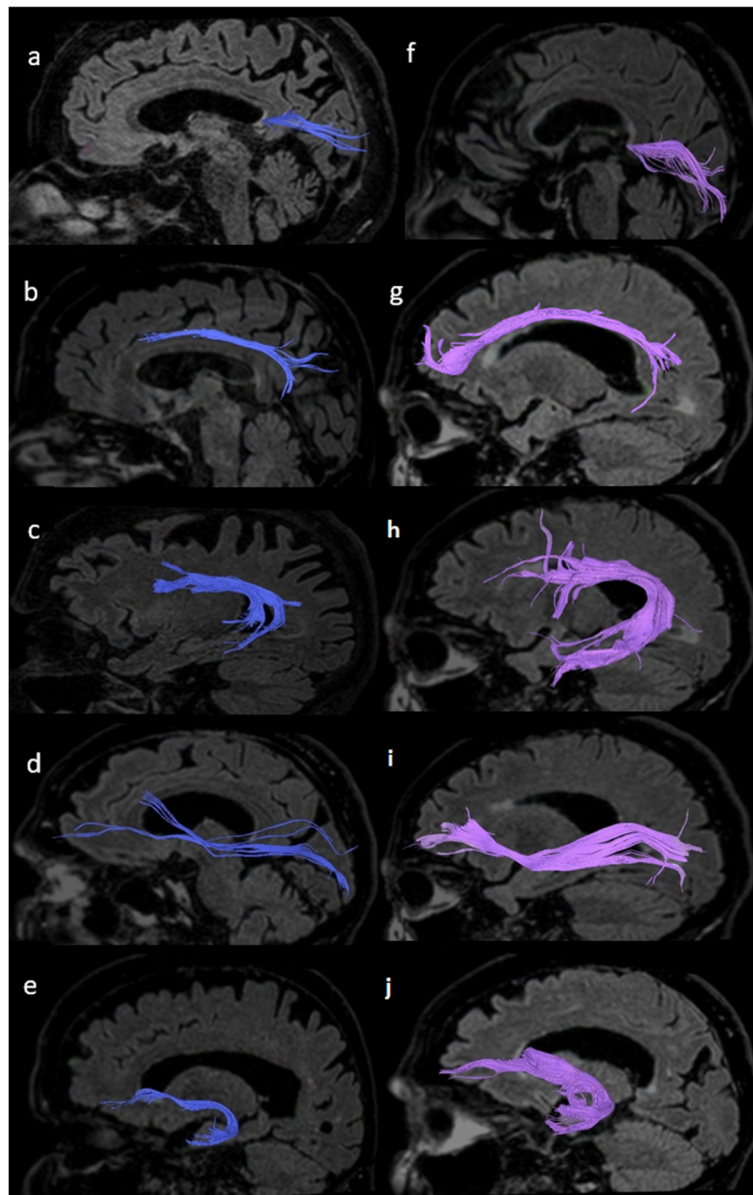


**Fig. 1** Example of the examined WM tracts in AD patients compared to healthy subjects. The examined tracts are shown on sagittal FLAIR-weighted images. White matter tracts of AD patients (**a–e**) are shown in blue color; while white matter tracts of the healthy subjects (**f–j**) are shown in purple color. **a, f** Splenium. **b, g** Cingulum. **c, h** Arcuate fasciculus. **d, i** Inferior fronto-occipital fasciculus. **e, j** Uncinate fasciculus. (Only tracts that revealed significant microstructural alteration are shown in this example). Significant differences were found in the MD of the splenium, right AF, right UF, and the IFOF bilaterally, between AD patients and healthy subjects. In addition, significant differences were found in FA of the cingulum bilaterally. AF, arcuate fasciculus; IFOF, inferior fronto-occipital fasciculus; UF, uncinate fasciculus; FA, fractional anisotropy; MD, mean diffusivity

100%, a specificity of 44% and an accuracy of 73% (Fig. 2e).

### Discussion

In the current study, dissection of WM tracts was performed via deterministic tractography, using the ROI approach, being less computationally extensive and more practical for clinical studies [17]. Overall, there were

significant differences in the FA of the cingulum, bilaterally, as well as in the MD of the splenium, right AF, right UF, and bilateral IFOF, between AD patients and control subjects. These findings reflect diffuse WM microstructural changes, likely representing degenerative changes, in AD [10].

The limbic system is a complex set of structures, lies on both sides of the thalamus just under the medial



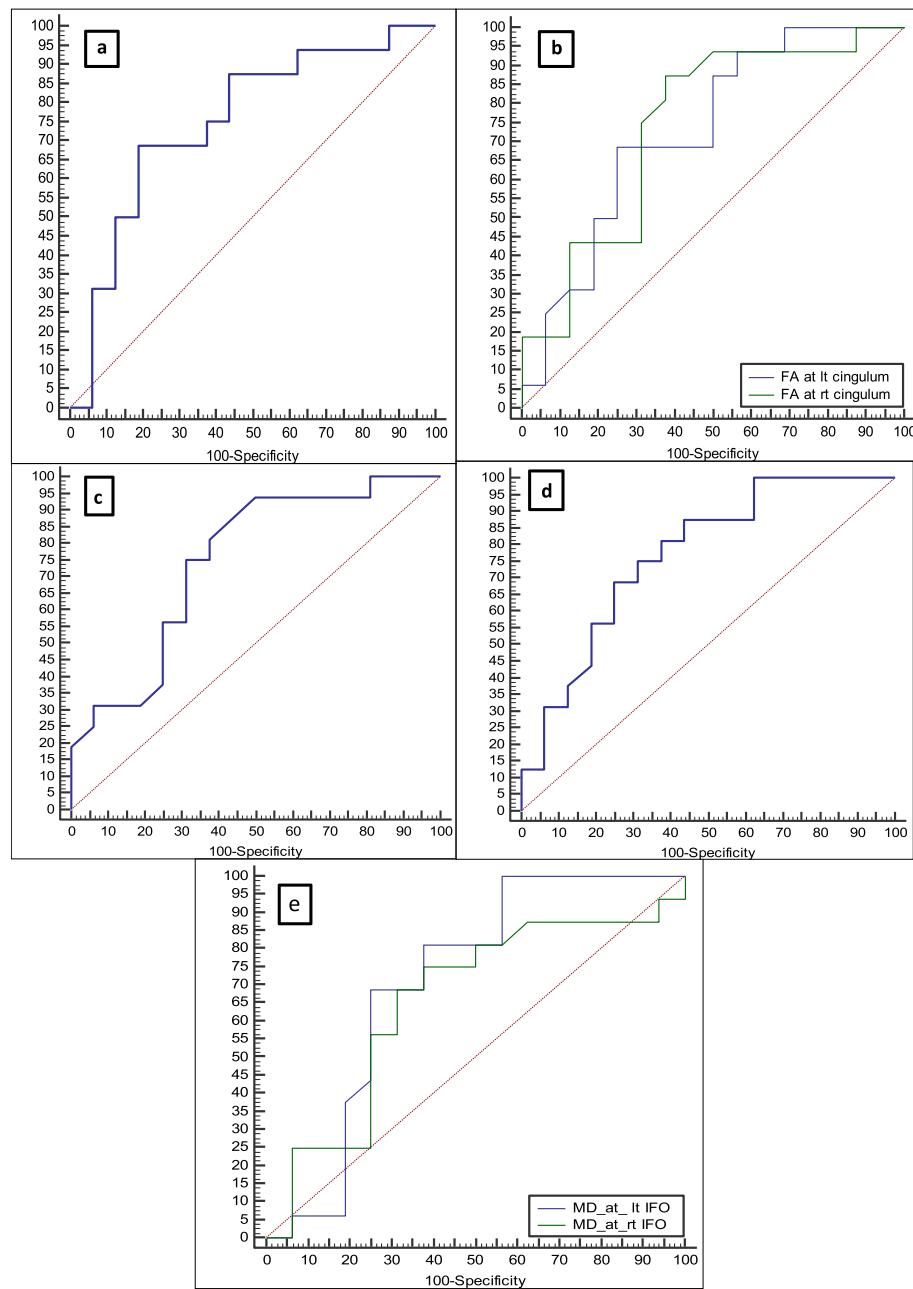


**Fig. 2** Diagnostic performance of **a** MD of the splenium, **b** FA of the cingulum, **c** MD of UF, **d** MD of AF, and **e** MD of IFOF in diagnosing AD. AF, arcuate fasciculus; IFOF, inferior fronto-occipital fasciculus; UF, uncinate fasciculus; FA, fractional anisotropy; MD, mean diffusivity

temporal lobes. It has been closely linked to emotions and memory and has shown to be the first affected part in AD [18]. The cingulum and fornix are the major WM fibers of the limbic system [19]. In the present study, there were significantly lower FA values in both right and left cingulum in AD patients relative to healthy controls. These findings are in agreement with DTI studies that revealed evident microstructural changes of the cingulum in AD [20, 21]. Furthermore, Lee et al. [22] found that, among the WM tracts, only the cingulum angular

fibers showed significant microstructural alteration in early AD compared to controls. These findings suggest that the cingulum is most affected by AD.

The fornix is another major component of the limbic system. Neurodegeneration of its fibers has been detected histologically in AD [23]. Accordingly, different DTI studies revealed significant microstructural changes of the fornix in the early stages of AD [24, 25]. However, in the present study, there were no significant differences in the DTI parameters of the fornix between AD

patients and control subjects. More advanced image acquisitions, which have been applied in the other studies, may be required for better estimation of the microstructural changes in such small tracts and to reduce the false-negative results. For instance, Mayo et al. [26] reported significant microstructural alteration in the fornix in AD relative to controls, when using 46 diffusion directions at a 3-T machine. Furthermore, the authors relied on probabilistic tractography in their analysis. The latter has been shown to be more accurate compared to deterministic tractography [27].

The corpus callosum is known to be involved in motor, somatosensory, and visual functions via inter-hemispheric transfer [28]. The current study demonstrated a significant increase in MD values of the splenium. Accordingly, Demey et al. [29] showed that all parts of the corpus callosum were adversely affected by AD. Yet, more consistent with the results of this study, Palesi et al. [30] reported that the splenium was predominantly affected by AD. These results may explain the poor motor, sensory, and visual output in AD patients.

The present study revealed significant higher MD of the right AF as well as significantly higher MD of the right UF in AD patients compared to healthy controls. Furthermore, there was higher MD of the IFOF bilaterally in AD patients compared to the controls. These results are in agreement with other cross-sectional DTI studies, investigating WM changes in AD patients compared to healthy subjects [31–33]. The damages of the above tracts are likely related to language, cognitive, and visual impairments with the progress of AD [32, 34, 35].

There were no significant differences, however, in DTI parameters of ILF and ATR between AD patients and healthy controls, in the current study. Although they were relatively preserved, a non-significant increase of MD values remains demonstrated in AD patients compared to healthy controls. Similarly, Niida et al. [36] revealed the absence of a significant difference in DTI parameters of ATR between AD patients and control subjects despite the visually depicted dissimilarity. In contrast to these results, Wegrzyn et al. [37] found a significant microstructural alteration of ATR and ILF in AD patients compared to control subjects. The small sample size, in this study, might be the reason behind the lack of significant results. Additionally, using different methodological approaches, e.g. deterministic tractography, may also contribute to these variations.

Regarding the diagnostic performance of the DTI parameters of the examined tracts, FA of the left cingulum showed the highest accuracy (81.8%). It is followed by FA of the right cingulum and MD of the splenium (77%) each. However, MD of the right IFOF showed the least accuracy (68.2%). Similarly, Jung et al. [38] also found that the cingulum had the best diagnostic performance

in differentiation between AD patients and healthy controls.

The small sample size is the main limitation in this study, which might make it difficult to generalize the results with confidence.

## Conclusion

Overall, the current study supports diffuse WM microstructural alteration in AD. In particular, the right UF, the right AF, and the splenium as well as the IFOF and cingulum, bilaterally, were significantly affected. The FA of the left cingulum provided the highest accuracy in differentiating AD from normal subjects. Thus, DTI parameters of the aforementioned tracts can act as a biomarker for the diagnosis of AD.

## Abbreviations

AD: Alzheimer's disease; AF: Arcuate fasciculus; ATR: Anterior thalamic radiation; CDR: Clinical Dementia Rating; DTI: Diffusion tensor imaging; FA: Fractional anisotropy; GM: Gray matter; IFOF: Inferior fronto-occipital fasciculus; ILF: Inferior longitudinal fasciculus; MD: Mean diffusivity; MMSE: Modified Mini-Mental State Examination; MRI: Magnetic resonance image; UF: Uncinate fasciculus; WM: White matter; ROI: Region of interest

## Acknowledgements

The study was supported by the Diagnostic Radiology Department, Assiut University.

## Authors' contributions

AMH, EMK, RKS, and SMA were responsible for the conception of the study design and data analysis. RKS and SMA contributed to the image interpretation and post-processing as well as manuscript writing. All authors have revised and approved the final manuscript.

## Funding

Not applicable

## Availability of data and materials

The datasets used and/or analyzed during the current study are available from the corresponding author on reasonable request.

## Declarations

### Ethics approval and consent to participate

The study was carried out after obtaining the permission of the Ethics Committee of Scientific Research, Faculty of Medicine, with IRB no. was 17101229. Informed verbal consent was waived as the study had no risk and does not affect the participants' rights as approved by the Ethics Committee of Scientific Research, Faculty of Medicine.

### Consent for publication

All patients included in this research gave written informed consent to publish the data contained within this study.

### Competing interests

The authors declare that they have no competing interests.

### Author details

<sup>1</sup>Department of Diagnostic and Interventional Radiology, Faculty of Medicine, Assiut University, Assiut, Egypt. <sup>2</sup>Department of Diagnostic Radiology, South Egypt Cancer Institute, Assiut University, Assiut, Egypt. <sup>3</sup>Department of Neuropsychiatry, Faculty of Medicine, Assiut University, Assiut, Egypt.

Received: 17 December 2020 Accepted: 11 March 2021

Published online: 30 March 2021

## References

1. Fratiglioni L, Wang HX (2007) Brain reserve hypothesis in dementia. *J Alzheimer's Dis* 12(1):11–22
2. Vos T, Allen C, Arora M et al (2016) Global, regional, and national incidence, prevalence, and years lived with disability for 310 diseases and injuries, a systematic analysis for the Global Burden of Disease Study. *The Lancet* 388(10053):1545–1602
3. Tarawneh R, Holtzman DM (2012) The clinical problem of symptomatic Alzheimer disease and mild cognitive impairment. *Cold Spring Harb Perspect Med* 2(5):a006148
4. Bateman RJ, Xiong C et al (2012) Clinical and biomarker changes in dominantly inherited Alzheimer's disease. *N Engl J Med* 367:795–804
5. Ribeiro LG, Busatto Filho G (2016) Voxel-based morphometry in Alzheimers disease and mild cognitive impairment: systematic review of studies addressing the frontal lobe. *Dement Neuropsychol* 10(2):104–112
6. Kim KW, MacFall J, Payne M (2008) Classification of white matter lesions on magnetic resonance imaging in elderly persons. *Biol Psychiatry*, 64, 273–280. <https://doi.org/10.1016/j.biopsych.03.024>.
7. Casella C (2020) Review: A critical review of white matter changes in Huntington's disease WM impairment in HD: secondary to, or independent of, neuronal degeneration? 35(8), 12–17. <https://doi.org/10.1002/mds.28109>.
8. Siger M, Schuff N, Zhu X et al (2009) Regional myo-inositol concentration in mild cognitive impairment using 1H magnetic resonance spectroscopic imaging. *Alzheimer Dis Assoc Disord*, 23(1), 57–62. <https://doi.org/10.1097/WA.0b013e3181875434>.
9. Bendlin BB, Carlsson CM, Johnson SC et al (2012) CSF T-TAU/A $\beta$  42 predicts white matter microstructure in healthy adults at risk for Alzheimer's disease. *PLoS One* 7(6):e37720
10. Croall ID, Lohner V, Moynihan B et al (2017) Using DTI to assess white matter microstructure in cerebral small vessel disease (SVD) in multicentre studies. *Clin Sci*;131:1361–1373. <https://doi.org/10.1042/CS20170146>.
11. Prados F, Boada I, Prats-Galino A et al (2010) Analysis of new diffusion tensor imaging anisotropy measures in the three-phase plot. *JMRI*, 31(6), 1435–1444. <https://doi.org/10.1002/jmri.22178>.
12. Mckhann G, Drachman D, Folstein M. et al (1984) Views & reviews. Clinica diagnosis of Alzheimer's disease: July.
13. Farrag A-KF, Farwiz H, Khedr E et al (1998) Prevalence of Alzheimer's disease and other dementing disorders: Assiut-Upper Egypt Study. *Dement Geriatr Cogn Disord*, 9, 323–328. <https://doi.org/10.1159/000017084>
14. Kaur S, Powell S, He L et al (2014). Reliability and repeatability of quantitative tractography methods for mapping structural white matter connectivity in preterm and term infants at term-equivalent age. 9(1). <https://doi.org/10.1371/journal.pone.0085807>
15. Kamali A, Flanders AE, Brody J et al (2014) Tracing superior longitudinal fasciculus connectivity in the human brain using high resolution diffusion tensor tractography. *Brain Struct Funct*, 219(1), 269–281. <https://doi.org/10.1007/s00429-012-0498-y>
16. Wakana S, Caprihan A, Panzenboeck MM et al (2007) Reproducibility of quantitative tractography methods applied to cerebral white matter. *NeuroImage*, 36(3), 630–644. <https://doi.org/10.1016/j.neuroimage.02.049>
17. Thompson PM, Zhan L (2015) Comparison of nine tractography algorithms for detecting abnormal structural brain networks in Alzheimer's Dis 7(April), 1–19. <https://doi.org/10.3389/fnagi.2015.00048>
18. Rajmohan V, Mohandas E (2007) The limbic system. *Indian J Psychiatry*, 49(2), 132–139. <https://doi.org/10.4103/0019-5545.33264>
19. Catani M, Thiebaut M, Schotten D (2008) A diffusion tensor imaging tractography atlas for virtual in vivo dissections. 44, 1105–1132. <https://doi.org/10.1016/j.cortex.2008.05.004>
20. Zhang Y, Schuff N, Jahng G-H et al (2007) Diffusion tensor imaging of cingulum fibers in mild cognitive impairment and Alzheimer disease. *Neurology*, 68(1), 13–19. <https://doi.org/10.1212/01.wnl.0000250326.77323.01>
21. Bozzali M, Giulietti G, Basile B et al (2012) Damage to the cingulum contributes to Alzheimer's disease pathophysiology by deafferentation mechanism. 1308, 1295–1308. <https://doi.org/10.1002/hbm.21287>
22. Lee S-H, Coutu J-P, Wilkens P et al (2015) Tract-based analysis of white matter degeneration in Alzheimer's disease. *Neuroscience* 301:79–89
23. Oishi K, Lyketsos CG (2014) Alzheimer's disease and the fornix. *Frontiers Aging Neurosci*, 6, 241. <https://doi.org/10.3389/fnagi.00241>
24. Oishi K, Mielke MM, Albert M et al (2012) The fornix sign: a potential sign for Alzheimer's disease based on diffusion tensor imaging. *J Neuroimaging* 22(4):365–374
25. Jin Y, Huang C, Daianu M et al (2017) 3D tract-specific local and global analysis of white matter integrity in Alzheimer's disease. 1207, 1191–1207. <https://doi.org/10.1002/hbm.23448>
26. Mayo CD, Garcia-barrera MA, Mazerolle EL et al (2019) Relationship between DTI metrics and cognitive function in Alzheimer's disease. 10(January).
27. Sarwar T (2019) Mapping connectomes with diffusion MRI : deterministic or probabilistic tractography? 1368–1384. <https://doi.org/10.1002/mrm.27471>
28. Schulte T, Müller-Oehring EM (2010) Contribution of callosal connections to the interhemispheric integration of visuomotor and cognitive processes. *Neuropsychol Rev*, 20(2), 174–190. <https://doi.org/10.1007/s11065-010-9130-1>
29. Demey I, Ventrice F, Rojas G et al (2015) Alzheimer's disease dementia involves the corpus callosum and the cingulum: a diffusion tensor imaging study (P6. 210).
30. Palesi F, De Rinaldis A, Vitali P et al (2018) Specific patterns of white matter alterations help distinguishing Alzheimer's and vascular dementia. *Frontiers Neurosci* 12:274
31. Ferris SH, Farlow M (2013) Language impairment in Alzheimer's disease and benefits of acetylcholinesterase inhibitors. *Clin Interv Aging*, 8, 1007–1014. <https://doi.org/10.2147/CIA.S39959>
32. Nestor PG, Kubicki M, Gurrera RJ et al (2004) Neuropsychological correlates of diffusion tensor imaging in schizophrenia. *Neuropsychology*, 18(4), 629–637. <https://doi.org/10.1037/0894-4105.18.4.629>
33. Kitamura S, Kiuchi K, Taoka T et al (2013) Longitudinal white matter changes in Alzheimer's disease: a tractography-based analysis study. *Brain Res*, 1515. <https://doi.org/10.1016/j.brainres.03.052>
34. Frye RE, Hasan K, Malmberg B et al (2010) Superior longitudinal fasciculus and cognitive dysfunction in adolescents born preterm and at term. *Dev Med Child Neurol*, 52(8), 760–766. <https://doi.org/10.1111/j.1469-8749.03633.x>
35. Kier EL, Staib LH, Davis LM et al (2004) MR imaging of the temporal stem: anatomic dissection tractography of the uncinate fasciculus, inferior occipitofrontal fasciculus, and Meyer's loop of the optic radiation. *May677–691*
36. Niida A, Niida R, Kuniyoshi K et al (2013) Usefulness of visual evaluation of the anterior thalamic radiation by diffusion tensor tractography for differentiating between Alzheimer's disease and elderly major depressive disorder patients. *Int J Gen Med*, 6, 189–200. <https://doi.org/10.2147/IJGM.S42953>
37. Wegrzyn M, Teipel SJ, Oltmann I et al (2012) Structural and functional cortical disconnection in Alzheimer's disease: a combined study using diffusion tensor imaging and transcranial magnetic stimulation. *Psychiatry Res*:1–9
38. Jung WS, Um YH, Kang DW et al (2018) Diagnostic validity of an automated probabilistic tractography in amnesic mild cognitive impairment. *Clin Psychopharmacol Neurosci*, 16(2), 144–152. <https://doi.org/10.9758/cpn.16.2.144>

## Publisher's Note

Springer Nature remains neutral with regard to jurisdictional claims in published maps and institutional affiliations.

**Submit your manuscript to a SpringerOpen<sup>®</sup> journal and benefit from:**

- Convenient online submission
- Rigorous peer review
- Open access: articles freely available online
- High visibility within the field
- Retaining the copyright to your article

Submit your next manuscript at ► [springeropen.com](https://www.springeropen.com)